Nuclear Overhauser Effect Studies of the Conformation of $Co(NH_3)_4ATP$ Bound to Kidney Na,K-ATPase†

John M. McD. Stewart,‡ Peter L. Jørgensen,§ and Charles M. Grisham*,‡

Department of Chemistry, University of Virginia, Charlottesville, Virginia 22901, and Institute of Physiology, University of Aarhus, 8000 Aarhus C, Denmark

Received June 29, 1988; Revised Manuscript Received February 7, 1989

ABSTRACT: Transferred nuclear Overhauser effect measurements (in the two-dimensional mode) have been used to determine the three-dimensional conformation of an ATP analogue, $Co(NH_3)_4ATP$, at the active site of sheep kidney Na,K-ATPase. Previous studies have shown that $Co(NH_3)_4ATP$ is a competitive inhibitor with respect to MnATP for the Na,K-ATPase [Klevickis, C., & Grisham, C. M. (1982) *Biochemistry 21*, 6979. Gantzer, M. L., et al. (1982) *Biochemistry 21*, 4083]. Nine unique proton–proton distances on ATPase-bound $Co(NH_3)_4ATP$ were determined from the initial build-up rates of the cross-peaks of the 2D-TRNOE data sets. These distances, taken together with previous ^{31}P and ^1H relaxation measurements with paramagnetic probes, are consistent with a single nucleotide conformation at the active site. The bound $Co(NH_3)_4ATP$ adopts an anti conformation, with a glycosidic torsion angle of 35°, and the conformation of the ribose ring is slightly N-type (C_2-exo, C_3-endo). The δ and γ torsional angles in this conformation are 100° and 178°, respectively. The nucleotide adopts a bent configuration, in which the triphosphate chain lies nearly parallel to the adenine moiety. Mn^{2+} bound to a single, high-affinity site on the ATPase lies above and in the plane of the adenine ring. The distances from enzyme-bound Mn^{2+} to N_6 and N_7 are too large for first coordination sphere complexes, but are appropriate for second-sphere complexes involving, for example, intervening hydrogen-bonded water molecules. The NMR data also indicate that the structure of the bound ATP analogue is independent of the conformational state of the enzyme. The TRNOE and paramagnetic probe techniques, two unique and independent spectroscopic measurements, thus provide a single, consistent picture of the structure of an ATP analogue at the active site of kidney Na,K-ATPase.

Na,K-ATPase[1] (sodium and potassium ion activated adenosine triphosphatase, EC 3.6.1.3) is the plasma membrane-bound protein that is responsible for the active extrusion of Na^+ and accumulation of K^+ by all mammalian cells. It consists of two polypeptides, a M_r 112 500 α subunit and a M_r 35 000 β subunit. The α subunit binds ATP and is covalently phosphorylated by ATP at Asp-369 in the catalytic cycle of the enzyme. The dimensions of the Na,K-pump molecule are known from analysis of crystals in the membrane (Jorgensen et al., 1982). Primary sequences for the α subunit from several different tissues and species have recently appeared (Shull et al., 1985). The availability of sequence information has generated considerable interest in the structure of this transport system and in the nature of the binding sites for ATP, the transported Na^+ and K^+ ions, and the divalent cation activator, Mg^{2+}. While much of this interest has centered on determining the protein residues involved in substrate and ion binding, our approach has focused primarily on the geometry and structure of the bound substrates and ions themselves.

Nuclear magnetic resonance methods have been widely used to determine the conformations and arrangement of enzyme-bound flexible substrates such as ATP (Sloan & Mildvan, 1976; Granot et al., 1979; Rosevear et al., 1983). Two NMR methods especially useful for these purposes are the paramagnetic probe T_1 method, which is used to measure metal–nucleus distances (Mildvan & Gupta, 1978; Mildvan et al., 1980), and the transferred nuclear Overhauser effect, which is used to measure relative and absolute interproton distances (Noggle & Schirmer, 1971; Tropp & Redfield, 1981; Mildvan et al., 1983; Clore & Gronenborn, 1982, 1983). The applications of both these methods have yielded mutually consistent conformations for ATP bound to protein kinase, for AMP bound to adenylate kinase, and for TTP and dATP bound to DNA polymerase, indicating the existence of unique nucleotide conformations on these enzymes (Granot, 1979; Rosevear et al., 1983; Fry et al., 1985; Ferrin & Mildvan, 1985, 1986).

We have previously shown that the substitution-inert Cr(III) and Co(III) analogues of ATP can be effective probes of nucleotide structure and function with Na,K-ATPase (O'Connor & Grisham, 1980; Grisham, 1981; Gantzer et al., 1982; Klevickis & Grisham, 1982). Kinetic studies (Gantzer et al., 1982) demonstrate that CoATP and CrATP are linear competitive inhibitors of Na,K-ATPase with respect to MnATP and MgATP under a variety of conditions. It has also been shown recently by one of us that Na,K-ATPase phosphorylated with CrATP strongly occludes up to 2.7 Na^+ and 2 K^+ per mole of phosphorylated ATPase (Vilsen et al., 1987). Using these complexes, we have previously established the existence of two divalent cation sites at the active site of the Na,K-ATPase (Grisham, 1981) and shown that these two sites are approximately 8.1 Å apart, as measured by Mn^{2+}

†Supported by grants from the National Institutes of Health (AM19419), the Muscular Dystrophy Association of America, the National Science Foundation, and the Danish Medical Research Council. The NMR instrumentation used in these studies was provided by grants from the National Science Foundation and the University of Virginia.

*To whom correspondence should be addressed.

‡University of Virginia.

§University of Aarhus.

[1] Abbreviations: Na,K-ATPase, sodium and potassium ion activated adenosinetriphosphatase; CoATP, β,γ-bidentate $Co(NH_3)_4ATP$; TMA, tetramethylammonium; Tes, 2-[[tris(hydroxymethyl)methyl]amino]-ethanesulfonic acid; Tris, tris(hydroxymethyl)aminomethane; NMR, nuclear magnetic resonance; EPR, electron paramagnetic resonance.

0006-2960/89/0428-4695$01.50/0

EPR (O'Connor & Grisham, 1980) and water proton measurements (A. O'Neal and C. Grisham, unpublished data). Recently, we have used the above-described paramagnetic probe T_1 method to determine the conformation of Co$(NH_3)_4$ATP bound at the active site of Na,K-ATPase (Stewart & Grisham, 1988; Grisham, 1988). Our data are consistent with an anti conformation for the adenine–ribose moiety of bound ATP and a C_2'-endo conformation for the ribose ring.

To corroborate these findings, we have now undertaken a series of transferred nuclear Overhauser effect measurements of Co$(NH_3)_4$ATP bound to Na,K-ATPase. The initial build-up rates of the cross-peaks in two-dimensional TRNOE studies can be used to calculate interproton distances for the bound substrate analogue. The distances determined in this study are fully consistent with the conformation of Co$(NH_3)_4$ATP determined from the paramagnetic probe T_1 method. This study is the first in which mutually consistent conformations have been obtained by these two methods for a membrane-bound enzyme.

Experimental Procedures

Materials. The β,γ-bidentate complex of Co$(NH_3)_4$ATP was prepared as described by Cornelius et al. (1977). ATP, NADH, phospho(enol)pyruvate, lactic dehydrogenase, and pyruvate kinase were purchased from Sigma. Tris-d_{11} was purchased from MSD Isotopes.

Enzyme Preparation. Kidneys obtained from freshly exsanguinated sheep at the Rocco Further Processing, Inc., of Timberville, VA, were frozen in dry ice and stored at −20 °C. The Na,K-ATPase was purified from the outer medulla of these kidneys as previously described (Jørgensen, 1974; O'Connor & Grisham, 1979). The ATPase activity was measured by the continuous method (Barnett, 1970), and only enzyme with a specific activity of more than 25 μmol of ATP hydrolyzed (mg of protein)$^{-1}$ min^{-1} at 37 °C was used in these experiments. Protein concentration was determined by the method of Lowry et al. (1951) using bovine serum albumin as a standard.

Solutions. In each 5-mm NMR tube, in a total volume of 600 μL, were present 3.0 mg/mL Na,K-ATPase, 10 mM β,γ-bidentate Co$(NH_3)_4$ATP, 15 mM Tris-d_{11} (pH 7.5 at 5 °C), 150 mM KCl or NaCl, and 0–5 mM $MnCl_2$. The water present was greater than 99% D_2O.

All stock solutions, except the ATPase and $MnCl_2$, were rigorously treated with Chelex 100 to remove divalent cations. The ATPase and Co$(NH_3)_4$ATP solutions were stored at −20 °C, while all other solutions were stored in a desiccator at 4 °C until use.

Stock D_2O–Chelex was prepared by lyophilization of Na^+– or K^+–Chelex 100 and reconstitution with 99.8% D_2O. Stock D_2O was prepared by column treatment of D_2O with D_2O–Chelex.

Tris buffers were prepared by dissolving Trizma 7.0 (Sigma, T3503) into D_2O. The 5 mM solutions, which had a pH of 7.5 ± 0.05 at 5 °C, were lyophilized and then stored in a desiccator at 4 °C. Deuterated Tris-d_{11} was prepared in a similar manner, adjusting the pH of small aliquots diluted to the desired concentration in H_2O at room temperature. β,γ-Bidentate Co$(NH_3)_4$ATP was prepared as described by Cornelius et al. (1977). Stock Co$(NH_3)_4$ATP was prepared by repeated rotary evaporation, replacing lost water with D_2O.

The Na,K-ATPase was prepared for the NMR experiments by diluting 1.8 mg of enzyme in 15 mL of an ice-cold solution of 10 mM Tris, pH 7.5, in D_2O and centrifuging at 25000g for 30 min at 4 °C. The pellet was resuspended in a small volume of ice-cold D_2O, buffered by Tris-d_{11}.

Nuclear Magnetic Resonance Experiments. Proton NMR spectra were obtained at 361 MHz on a Nicolet Magnetics Corp. NT-360/Oxford spectrometer equipped with a 1200/293B data system. The spectra were measured at 4 °C with a 5-mm proton probe and deuterium lock. The 90° pulse width was typically 7.50–7.75 μs at 361 MHz. The HDO signal was decoupled during delays prior to the pulse sequences. The typical experiment collected 16 accumulations of 128 blocks of 512 data points, for each of 5 to 6 mixing times per sample. Fourier transformed data were zero-filled such that two-dimensional spectra consisted of 512 blocks of 1K data. Data collection for each mixing time required about 2 h.

Initial build-up rates of primary NOEs were measured in a phase-sensitive two-dimensional NOE experiment (States et al., 1982). Rates were determined by fitting a straight line to the data of a cross-peak intensity vs mixing time plot, employing mixing times not greater than 100 ms. For each proton–proton interaction in the five high-KCl and five high-NaCl titrations, weighted averaging of the slopes of the lines fitted to the cross-peak intensity vs mixing time data determined the mean initial build-up rate and its uncertainty. All line fitting was done with the use of the program NONLIN (courtesy of Dr. Michael Johnson, Department of Pharmacology, University of Virginia Medical School).

In a 2D NOE experiment, diagonal peaks represent magnetization that has not been exchanged. Cross-peaks result from the exchange of magnetization through dipole–dipole cross-relaxation. The integrated intensity of each resonance in a two-dimensional spectrum is proportional to a mixing coefficient, which is a function of the mixing time, t_m (analogous to the length of the irradiation pulse in the 1D NOE experiment). In a phase-sensitive 2D NOE experiment, negative "enhancements" or NOEs in the 1D experiment are seen as positive cross-peaks. Positive enhancements are seen as negative cross-peaks. Approximate distances can be obtained from the cross-peak build-up rate, $\eta(t_m)$, by assuming that it is directly proportional to the cross-relaxation rate, which is only true in the limit as t_m approaches zero (and under the assumption that the same correlation time applies for both interactions).

$$\frac{r_{ij}}{r_{kl}} \approx \left(\frac{\eta_{kl}(t_m)}{\eta_{ij}(t_m)}\right)^6 \qquad (1)$$

Transferred nuclear Overhauser enhancements (TRNOE) can occur in the case of an enzyme with excess substrate in chemical exchange. Substrate free in solution is characterized by a short rotational correlation time, so that $\omega^2\tau_r^2 \ll 1$ and the observed cross-peaks are positive. Substrate bound to protein is characterized by the large rotational correlation time of the macromolecule, such that $\omega^2\tau_r^2 \gg 1$ and the observed cross-peaks (arising from intramolecular NOEs) would be negative. Chemical exchange effectively transfers magnetization from the bound state to the free state. When chemical exchange is fast on the cross-relaxation rate scale, then the observed cross-relaxation rate is the weighted average of the cross-relaxation rates in the free and bound states. The theory of NOE and TRNOE methods in one- and two-dimensional modes has been described in detail elsewhere (Solomon, 1955; Noggle & Schirmer, 1971; Bothner-By, 1979; Macura & Ernst, 1980; Clore & Gronenborn, 1982, 1983; Keepers & James, 1984; Bremer et al., 1984; Perrin & Gipe, 1984; Olezniczak et al., 1986).

Distances were determined by using the average H_1'–H_2' cross-peak initial build-up rate as a reference, assuming that it described a distance of 2.9 ± 0.1 Å (Rosevear et al., 1983).

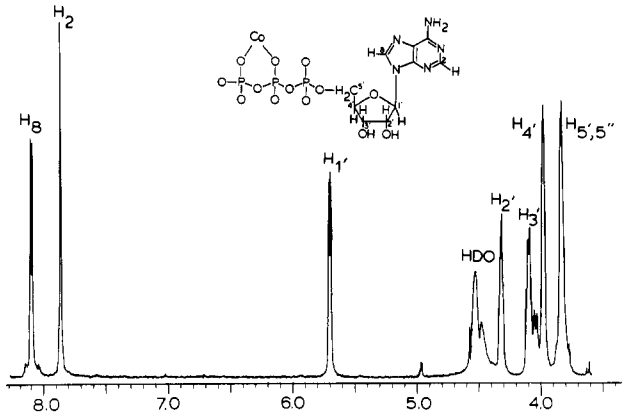

FIGURE 1: Hydrogen (H-1) NMR spectrum of $Co(NH_3)_4ATP$ at 361 MHz at pH 7.5, 4 °C. Chemical shifts are relative to DSS. The solution contained D_2O (99+%), and the residual water signal was irradiated to reduce its intensity.

RESULTS

Phase-Sensitive NOE Measurements. ^1H transferred nuclear Overhauser effects for the protons of $Co(NH_3)_4ATP$ were measured in solutions of Na,K-ATPase at 361 MHz. The 361-MHz ^1H NMR spectrum of $Co(NH_3)_4ATP$ in the presence of kidney Na,K-ATPase is shown in Figure 1. The resonances are labeled in the conventional manner. In this particular sample, $Co(NH_3)_4ATP$ was dissolved in D_2O (99.8%). The residual HDO signal appears at 4.99 ppm relative to DSS at 4 °C. At 23 °C, it appears at 4.79 ppm relative to DSS. All the NMR experiments described here were performed at 4 °C to ensure enzyme stability. An unexpected benefit of the lower temperature is the downfield shift of the HDO resonance that is sufficient to expose a well-resolved $H_{2'}$ resonance at 361 MHz, which is obscured by the water signal at temperatures above 15 °C. The NH_3 protons of $Co(NH_3)_4ATP$ were exchanged for deuterons by raising the pD of the solution to 9.0 for a few minutes. Nevertheless, there remains in this spectrum a small signal (the doublet at 4.52 ppm) from the *cis*-NH_3, which exchange more slowly than do the *trans*-NH_3. Reports describing the advantages of phase-sensitive two-dimensional NOE measurements have appeared (States et al., 1982). The result of a phase-sensitive experiment with CoATP in the presence of Na,K-ATPase is seen in Figure 2. In addition to the expected ribose proton cross-peaks, the H_8–$H_{2'}$ cross-peak is clearly visible in this positive map, while no coherent cross-peak signals are seen in the negative map. Deoxygenated solutions of CoATP in the absence of Na,K-ATPase normally produce negative cross-peaks (data not shown). In the absence of enzyme, no cross-peaks were visible in these studies. These results indicate that the dipole–dipole relaxation of CoATP bound to the protein is transferred to the free CoATP through chemical exchange. Therefore, the build-up rates of cross-peak intensity measured in this experiment on the free CoATP signal can be used to calculate proton–proton distances of protein-bound CoATP.

The diagonal blocks of a 2D spectrum are shown in Figure 3. The mixing time used in these experiments was 100 ms, which is approximately the time necessary for maximal primary cross-peak development. Nevertheless, no cross-peaks appear in the H_2 diagonal block, consistent with an anti conformation for the adenine moiety of the bound CoATP.

Build-Up Rates of the 2D-TRNOE Cross-Peaks. The intensities of the cross-peaks of the 2D-TRNOE spectra (Figure 2) can be measured as a function of mixing time. A plot of such measurements for the three strongest interactions,

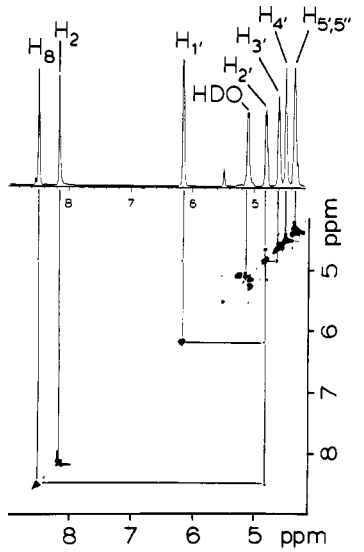

FIGURE 2: 2D-TRNOE contour plot (phase-sensitive mode) of CoATP in solution of Na,K-ATPase. Conditions were as described in Figure 1. The pulse sequence was as previously described (States et al., 1982).

Table I: Build-Up Rates of Cross-Peak Intensities and Proton–Proton Distance Ratios Calculated from the 2D-TRNOE Measurements

proton pair	Na^+ form	K^+ form	av	distance ratio[a]
H_8–$H_{1'}$	0.27 ± 0.02	0.24 ± 0.02	0.26 ± 0.02	1.2 ± 0.1
H_8–$H_{2'}$	0.78 ± 0.07	0.67 ± 0.04	0.70 ± 0.04	1.1 ± 0.1
H_8–$H_{3'}$	0.27 ± 0.03	0.26 ± 0.02	0.26 ± 0.02	1.2 ± 0.1
H_8–$H_{4'}$	0.20 ± 0.02	0.15 ± 0.02	0.16 ± 0.02	1.3 ± 0.1
H_8–$H_{5',5''}$	0.19 ± 0.02	0.23 ± 0.03	0.20 ± 0.02	1.3 ± 0.3
$H_{1'}$–$H_{2'}$	1.0	1.0	1.0	1.0
$H_{1'}$–$H_{3'}$	0.21 ± 0.02	0.18 ± 0.02	0.20 ± 0.02	1.3 ± 0.1
$H_{1'}$–$H_{4'}$	0.35 ± 0.04	0.28 ± 0.02	0.30 ± 0.02	1.2 ± 0.1
$H_{1'}$–$H_{5',5''}$	0.16 ± 0.02	0.14 ± 0.02	0.15 ± 0.02	1.4 ± 0.2

[a] Average (between Na^+ and K^+ conditions) ratio of initial build-up rates were used to calculate proton–proton distance ratios. All rates and distance ratios were calculated relative to $H_{1'}$–$H_{2'}$ interaction. Uncertainties in distances for $H_{5',5''}$ protons were greater than others due to orientational uncertainties. It can be seen from inspection of models that the H_8–$H_{4'}$ and $H_{1'}$–$H_{5',5''}$ interactions involve contributions from spin diffusion.

$H_{1'}$–$H_{2'}$, H_8–$H_{2'}$, and H_8–$H_{1'}$, is shown in Figure 4. (The $H_{2'}$–$H_{3'}$ interaction is actually the strongest. However, the proximity of the two resonances creates overlap and base-line modulations that make accurate measurements of cross-peak intensity difficult. This is why $H_{1'}$ is the only ribose resonance used to determine intra-ribose distances.) This plot represents data from two separate experiments, using open and solid symbols to distinguish the two. The error bars shown include data from both upper and lower cross-peaks, since the data set is symmetric about the diagonal. The cross-peak intensities increase monotonically and more or less linearly for mixing times less than 100 μs and then either level off (H_8–$H_{3'}$ and H_8–$H_{2'}$) or decrease with increasing times ($H_{1'}$–$H_{2'}$), indicating that spin–lattice relaxation, ρ, has begun to dominate the cross-peak build-up curve.

Distance Determinations. Initial build-up rates for cross-peak intensity were determined by fitting a line (using the program NONLIN) to the data in each experiment. The rates and errors in rate were determined for each interaction. For each experiment, the ratio of each build-up rate to the rate determined for the $H_{1'}$–$H_{2'}$ interaction in that same experiment was determined. Weighted averaging by relative size of error was performed. Table I lists the build-up rates of the cross-peak intensities for the Na^+ and K^+ experiments and the distance ratios. The important assumption that is made here

Table II: Paramagnetic Contributions to Relaxation Rates at 300 and 361 MHz for Protons of $Co(NH_3)_4ATP$ and Mn^{2+}–H Distances in the ATPase-Bound Mn^{2+}–$Co(NH_3)_4ATP$ Complex

	H_8	H_2	$H_{1'}$	$H_{2'}$	$H_{3'}$	$H_{4'}$	$H_{5',5''}$
$1/T_{1M}$[a]	17000–37600	1410–1530	730–770	1650–1810	1250–1390	620–690	710–800
r_{Mn-H}[b] (Å)	4.3–4.9	7.4 ± 0.1	8.2 ± 0.1	7.2 ± 0.1	7.5 ± 0.1	8.4 ± 0.1	8.2[c]

[a] Using $1/\tau_M = 1.395\ (\pm 0.275) \times 10^4$ (Stewart & Grisham, 1988), reported by range of values. [b] Using $\tau_c = 5.47\ (\pm 0.40) \times 10^{-10}$ (Stewart & Grisham, 1988). [c] Only an approximate distance, due to orientational uncertainties.

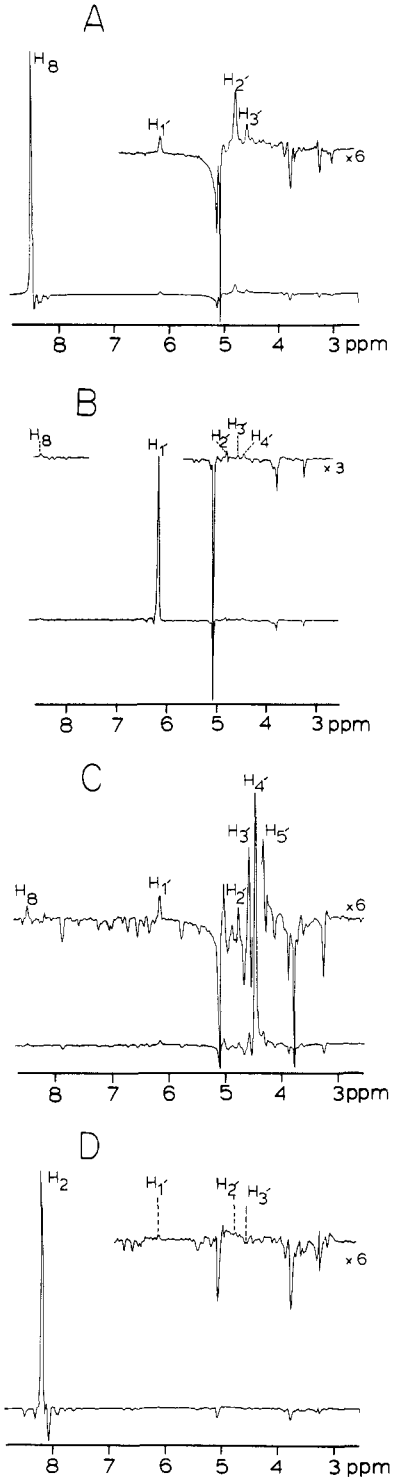

FIGURE 3: Single spectra taken from the data set of Figure 2. Spectra are expanded, and cross-peak positions are labeled. The strongest resonance signal in each spectrum (A, H_8; B, $H_{1'}$; C, $H_{4'}$; and D, H_2) is the resonance from the diagonal in Figure 2.

is that the same correlation time, τ_r, that characterizes the $H_{1'}$–$H_{2'}$ interaction also characterizes all other measured interactions.

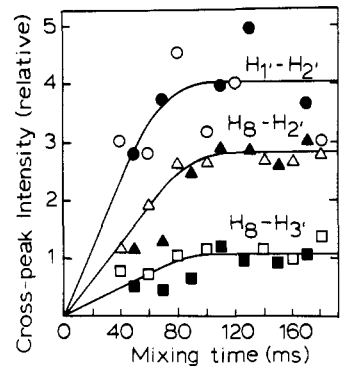

FIGURE 4: Buildup of intensity of cross-peaks from 2D-TRNOE spectra as shown in Figure 3 as a function of mixing time for three proton–proton interactions. The data represent the results of two experiments, distinguished by open and solid circles.

To correctly interpret the rates of cross-peak intensity development, it is important to know that there is negligible negative contribution to the positive cross-peaks from CoATP free in solution. This is known by the observation that only degassed solutions of CoATP alone (no enzyme present) provide 2D NOE maps with any negative cross-peak intensity. Nondegassed solutions of CoATP do not show cross-peaks. Apparently, in the absence of Na,K-ATPase, interactions between CoATP and paramagnetic dissolved O_2 provide the major relaxation pathway, so that no NOEs are observed. NMR solutions of enzyme and CoATP were never degassed. The major relaxation pathway of this solution is due to interaction with the protein. The conformation of protein-bound CoATP determined from positive cross-peak intensity development, therefore, must have only negligible contributions from whatever conformations of CoATP exist in solution.

Comparison of E_1 and E_2 Conformations of Na,K-ATPase. The phase-sensitive experiment was repeated five times each for the high-Na^+ and the high-K^+ conditions as described under Experimental Procedures, in the hopes of eliciting any cationic-dependent conformational differences in Na,K-ATPase, as described above. The data (Table I) indicate no significant conformational differences for the adenosine moiety of protein-bound CoATP when Na^+ is replaced by K^+. This is fully consistent with previous paramagnetic relaxation experiments using CoATP (Stewart & Grisham, 1988).

Discussion

Conformational analysis was done on a Silicon Graphics computer using the program MMS (copyright UCSD). $Co(NH_3)_4ATP$ was constructed from the X-ray data of rubidium adenosine 5′-diphosphate monohydrate (Viswamitra et al., 1976) and $Co(NH_3)_4H_2P_3O_{10}\cdot H_2O$ (Merritt et al., 1978). Protons were attached to the structure "by hand", using proper bond lengths and approximating tetrahedral geometry. The results of the paramagnetic probe (Stewart & Grisham, 1988) and TRNOE studies (Tables I and II) are consistent with a model for the active site in which the nucleotide is U-shaped and the Mn^{2+} is above and approximately planar with the adenine ring. This model is shown in Figure 5. To model the TRNOE data, a value for the $H_{1'}$–$H_{2'}$ distance had to be

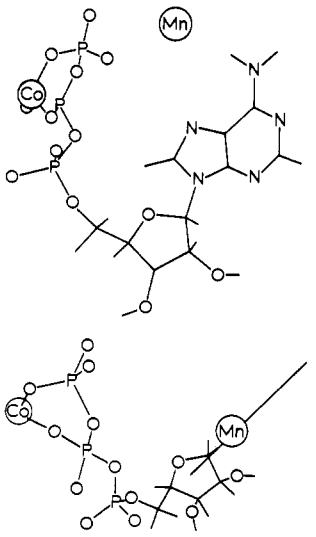

FIGURE 5: Conformation of $Co(NH_3)_4ATP$ and the enzyme-bound Mn^{2+} ion at the active site of kidney Na,K-ATPase. The structure was derived on a Silicon Graphics workstation using MMS software with the distances determined from the magnetic resonance experiments. The Mn^{2+}–Co^{3+} distance is taken as that obtained with Cr^{3+} by Mn^{2+} EPR (O'Connor & Grisham, 1980). All other distances were determined from the 2D-TRNOE relaxation data presented here and the paramagnetic relaxation data previously described (Stewart & Grisham, 1988). These latter distances were calculated by using a dipolar correlation time of 5.47×10^{-10} s.

assumed. This distance can vary from 2.5 Å in the 3′-endo sugar conformation to 2.9 Å in the 2′-endo conformation. In the model shown in Figure 5, a value of 2.9 Å was used, since, as pointed out below, our data are most consistent with the 3′-endo conformation. The conformation of the $Co(NH_3)_4ATP$ has the glycosidic bond linking the adenine base to the ribose sugar in the anti conformation. The sequence of atoms defining the angle is O_4–C_1–N_9–C_4. The torsional angle about the C_1–N_9 bond that links base to sugar is denoted by χ. The term anti refers to the values of χ in the range 0° ± 90°. Syn refers to angles of 180° ± 90° degrees (Davies, 1978). The value of χ determined from model building is 35° ± 10°. The anti configuration is much more generally found in purine nucleotides and their complexes in the crystalline state as well as in solution (Saenger, 1984).

As shown in Figure 6, the conformation of the ribose ring is slightly N-type ($C_{2'}$ is exo and $C_{3'}$ is endo). In solution, purine ribosides normally show a small conformation preference for the S-type conformer ($C_{2'}$ is endo and $C_{3'}$ is exo) (Altona & Sundaralingam, 1973). The torsional angle δ is indicative of the puckering in the ribose and is defined by the atom sequence $C_{5'}$–C_4–$C_{3'}$–$O_{3'}$ (Saenger, 1984). The value mesured for protein-bound CoATP is 101° ± 10°. The orientation of $O_{5'}$ relative to the ribose ring is determined by the torsional angle γ, defined by the sequence $O_{5'}$–$C_{5'}$–$C_{4'}$–$C_{3'}$ (Saenger, 1984). The value measured in the present model is 178° ± 10°, a typical value for protein-bound MgATP (Fry et al., 1985). Figure 6 illustrates the conformation of CoATP in terms of χ, δ, and γ.

The agreement between the previous paramagnetic probe relaxation studies (Stewart & Grisham, 1988) and the present TRNOE measurements is encouraging. It has not previously been possible to make comparisons of this type, even though several NMR investigations of the active-site structure of Na,K-ATPase have appeared (Klevickis & Grisham, 1982; Grisham et al., 1974; Grisham & Mildvan, 1974, 1975; Grisham, 1981). The structural information derived from each technique argues convincingly for an anti conformation for

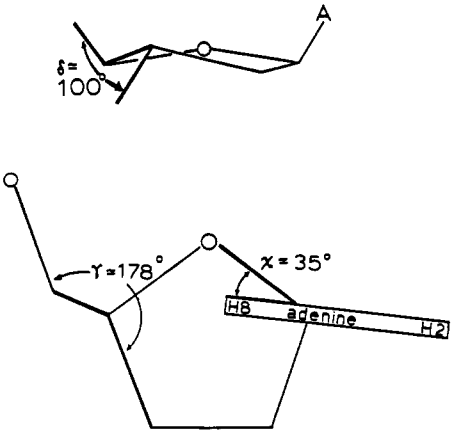

FIGURE 6: Two views of the ribose ring of CoATP bound to Na,K-ATPase. The structure is derived from the distances calculated from the 2D-TRNOE data (Table II) and the previously described paramagnetic relaxation measurements in Table III. The torsional angles χ, δ, and γ are shown for the bound CoATP.

Table III: Some Protein-Bound Nucleotide Conformations

enzyme	substrate		γ (deg)	δ (deg)	χ (deg)
Na,K-ATPase	$Co(NH_3)_4ATP$		180	100	33
adenylate kinase[a]	AMP		180	105	110
	MgATP		170	97	65
adenylate kinase fragment[b]	MgATP		50	94	60
protein kinase[c]	$Co(NH_3)_4ATP$				78
creatine kinase[d]	MgATP				78
pyruvate kinase[e]	MgATP (site 2)			90	68
	MgATP (site 1)	62%		(C_3-endo	30)
		20%		(O_1-endo	55)
		18%		(C_2-endo	217)
large fragment of DNA polymerase I in the presence of template[f]	MgdATP			90	62
	MgTTP			100	40
	MgdGTP	60%		(90	32)
		40%		(144	222)
	MgUTP			105	60

[a] Fry et al. (1985, 1987). [b] Fry et al. (1985). [c] Granot et al. (1979); Rosevear et al. (1983). [d] Rosevear et al. (1987a). [e] Rosevear et al. (1987b). [f] Ferrin and Mildvan (1985, 1986).

the bound nucleotide. No cross-peaks involving the adenine H_2 proton could be detected in the present study, and the seven Mn–H distances measured in the paramagnetic probe experiments (Table II) can only be fit by an anti conformation. The paramagnetic probe relaxation measurements are also consistent with the notion that the enzyme-bound divalent cation lies above and in the plane of the adenine ring of bound $Co(NH_3)_4ATP$. The similarity between this structure and that determined by X-ray crystallography for transition-metal complexes of 1,9-disubstituted adenine derivatives (Chiang et al., 1979) is interesting. Chiang et al. describe two possible chelation models for a metal interacting with the N_7 and N_6 positions of adenine. As shown in Figure 7, in their neutral imino form I, adenine nucleotides are capable of acting either as bidentate chelating agents, employing the lone pair density at the endocyclic N_7 site and the exocyclic imino group N_6H, or in a monodentate mode with N_7 as the sole binding site and with the possible utilization of the imino proton as a hydrogen-bond donor. In the protonated form II, N_7 is the primary metal binding site and the exocyclic amino group acts as a hydrogen-bond donor to acceptor sites on the ligands (H_2O, for example) in the primary coordination sphere of the metal center. In the structure of the bound CoATP, Mn^{2+} appears to be approximately planar with the adenine and above N_7 and N_6. The distance to N_7 is 3 Å in this model, too far for a first coordination sphere complex. However, the similarity between

Table IV: Sequence Homologies of Segments Contributing to Nucleotide Binding Domains in Adenylate Kinase and Phosphofructokinase with Na,K-ATPase and Other Cation-Pump Proteins in Plasma Membranes

sequence (with beginning residue number shown)																			enzyme	ref
104	E	F	E	R	K	-	I	G	Q	P	T	L	L	L	Y	V	D	A	G	P	adenylate kinase	Fry et al. (1985)
87	E	Q	L	K	K	-	H	G	I	Q	G	L	V	V	I	G	G	D	G	S	phosphofructokinase	Kolb et al. (1980)
543	L	G	E	R	V	-	L	G	F	C	H	L	F	L	P	D	E	Q	F	P	Na,K-ATPase, α	Kawakami et al. (1986)
613	L	K	C	R	T	-	A	G	I	R	V	I	M	V	T	G	D	H	P	I	H,K-ATPase	Shull and Lingrel (1986)
611	Q	L	C	R	D	-	A	G	I	R	V	I	M	I	T	G	D	N	K	G	Ca-ATPase	Brandl et al. (1986)

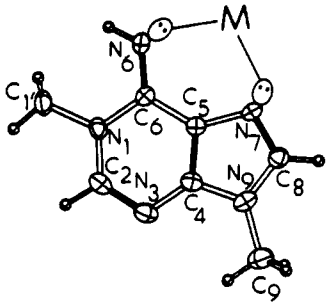

I

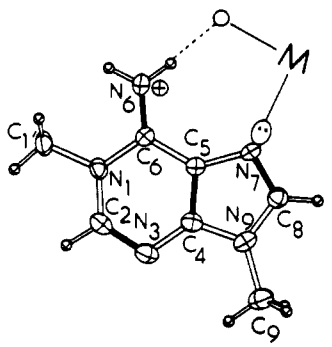

II

FIGURE 7: Structures described by Chiang et al. (1979) in crystallographic studies of Co(III) complexes of 1,9-dimethyladeninium cation.

the structures is striking. A reasonable speculation is interaction between the divalent metal and N_7 and N_6 of adenine via water.

Table III lists nucleotide conformations determined by TRNOE or paramagnetic probe studies for some enzyme systems. Results obtained for certain enzymes require fitting experimental data to multiple conformations. This is not required by the present results. It is also seen that the conformation determined for Na,K-ATPase most closely resembles that of MgATP bound to adenylate kinase. However, the difference in χ between the two is significant. In fact, it would appear that Na,K-ATPase is unusual by virtue of its low value for χ of bound substrate. On the other hand, Na,K-ATPase, being a membrane-bound protein, is unlike the other proteins of Table III.

Mildvan (1974) has proposed several generalities on enzyme mechanisms, among which he states that enzymes that alter or restrict the glycosidic torsional angles of nucleotide substrates to values different from those found in the unbound substrate also show high nucleotide substrate specificities, both effects probably resulting from the same steric interactions (Mildvan, 1981). The Na,K-ATPase can substitute several nucleotides for ATP, although less effectively. The maximal rate of hydrolysis and the activating effect of nucleotide hydrolysis on K^+-dependent phosphatase follow the same pattern of ATP > CTP > ITP > GTP ≥ UTP (Boldyrev et al., 1982, 1984). CTP exhibits the same complicated kinetics, with two apparent K_m values, as does ATP. GTP and UTP each have a single K_m value, while ITP exhibits an intermediate behavior. Svinukhova and Boldyrev (1987) have measured ouabain-sensitive Na^+ accumulation into proteoliposomes with reconstituted Na,K-ATPase. They attribute the effectiveness of the nucleotide in Na,K-ATPase function to the pK_a of the N_1 (N_3) atom of the purine (pyrimidine) base; those nucleotides that can accept a proton at neutral pH are the most efficient substrates. It is expected that hydrogen-bond formation between a residue of the protein [perhaps one of the two histidyl residues implicated at the active site (Miara et al., 1985)] and N_1 of adenine would restrict ATP to a single glycosyl conformation, while enabling effective CTP binding.

An important feature of the ATP binding domain in adenylate kinase is a hydrophobic pocket formed by Ile, Val, His, and Leu residues for accommodation of adenine and ribose moieties. Table IV demonstrates homology with respect to the position of charges and hydrophobic residues between adenylate kinase and phosphofructokinase on one hand and α subunit of Na,K-ATPase and the two other cation-pump proteins H,K-ATPase and Ca-ATPase. In adenylate kinase, this segment forms a hydrophobic strand of parallel β-pleated sheet terminated by an aspartate that flanks the triphosphate chain of MgATP (Fry et al., 1985).

Other segments without homology to adenylate kinase participate in formation of the nucleotide binding domain in the cation-pump proteins. In addition to the segment around the residue for covalent phosphorylation from ATP (Asp-369 in α subunit of Na,K-ATPase), labeling with ATP analogues provides evidence for segments around residues that are labeled by FITC (Karlish, 1980), FSBA (Ohta et al., 1986), and CIR-ATP (Ovchinnikov et al., 1985). These segments show high homology between cation-pump proteins with respect to both amino acid sequence and tertiary organization of the segments relative to transmembrane helical segments. They show no resemblance to other sequences contributing to formation of nucleotide binding site in adenylate kinase.

The sequence data complement the present results, demonstrating a partial resemblance of the conformation of ATP bound in adenylate kinase to that in Na,K-ATPase. Part of the ATP moiety is organized in a manner similar to that in adenylate kinase, while there is a significant difference in torsion angle about the bond between adenine and ribose. This agrees with the homology between amino acid sequences belonging to the backbone of the nucleotide binding sites, while other parts of the domain, probably involved in more specific cation-dependent reactions and ion translocation, are specific for the cation-pump proteins.

ACKNOWLEDGMENTS

We acknowledge the generous and invaluable help of Nancy Cook of Rocco Further Processing, Timberville, VA, and the excellent technical assistance of Jaymee P. Girard.

REFERENCES

Altona, A., & Sundaralingam, M. (1973) *J. Am. Chem. Soc. 95*, 2333.

Barnett, R. (1970) *Biochemistry 9*, 4644.

Boldyrev, A. A., & Svinukhova, I. A. (1982) *Biochim. Biophys. Acta 707*, 167.
Boldyrev, A. A., Lopina, O. D., Gulyaev, N. N., Baranova, L. A., & Severin, E. S. (1984) *FEBS Lett. 175*, 303.
Bothner-By, A. A. (1979) in *Biological Applications of Magnetic Resonance* (Shulman, R. G., Ed.) p 177, Academic Press, New York.
Brandl, C. J., Green, N. M., Korczak, B., & MacLennan, D. H. (1986) *Cell 44*, 597–607.
Bremer, J., Mendz, G. L., & Moore, W. J. (1984) *J. Am. Chem. Soc. 106*, 4691.
Chiang, C. C., Epps, L. A., Marzilli, L. G., & Kistenmacher, T. J. (1979) *Inorg. Chem. 18*, 791.
Clore, G., & Gronenborn, A. (1982) *J. Magn. Reson. 48*, 402–417.
Clore, G., & Gronenborn, A. (1983) *J. Magn. Reson. 53*, 423–442.
Cornelius, R., Hart, P., & Cleland, W. (1977) *Inorg. Chem. 16*, 2799.
Davies, D. B. (1978) *Prog. NMR Spectrosc. 12*, 135.
Ferrin, L., & Mildvan, A. (1985) *Biochemistry 24*, 6904–6913.
Ferrin, L., & Mildvan, A. (1986) *Biochemistry 25*, 5131–5145.
Fry, D., Kuby, S., & Mildvan, A. (1985) *Biochemistry 24*, 4680–4694.
Fry, D. C., Kuby, S. A., & Mildvan, A. S. (1987) *Biochemistry 26*, 1645.
Gantzer, M., Klevickis, C., & Grisham, C. (1982) *Biochemistry 21*, 4083.
Granot, J., Kondo, H., Armstrong, R., Mildvan, A., & Kaiser, E. (1979) *Biochemistry 18*, 2339–2345.
Grisham, C. (1981) *J. Inorg. Biochem. 14*, 45.
Grisham, C. (1988) *Methods Enzymol. 156*, 353–371.
Grisham, C. M., & Mildvan, A. (1974) *J. Biol. Chem. 249*, 3187.
Grisham, C. M., & Mildvan, A. (1975) *J. Supramol. Struct. 3*, 304.
Grisham, C. M., & Hutton, W. (1978) *Biochem. Biophys. Res. Commun. 81*, 1406.
Grisham, C. M., Gupta, R., Barnett, R., & Mildvan, A. (1974) *J. Biol. Chem. 249*, 6738.
Jeener, J., Meier, B. H., Bachman, P., & Ernst, R. R. (1979) *J. Chem. Phys. 71*, 4546.
Jorgensen, P. L. (1974) *Methods Enzymol. 32*, 277.
Jorgensen, P. L., Skriver, S., Hebert, H., & Maunsbach, A. B. (1982) *Ann. N.Y. Acad. Sci. 420*, 203.
Karlish, S. J. D. (1980) *J. Bioenerg. Biomembr. 12*, 111–136.
Kawakami, K., Nojima, H., Ohta, T., Nagano, K. (1986) *Nucleic Acids Res. 14*, 2833–2844.
Keepers, J. W., & James, T. L. (1984) *J. Magn. Reson. 57*, 404.
Klevickis, C., & Grisham, C. (1982) *Biochemistry 21*, 6979.
Kolb, E., Hudson, P. J., & Harris, J. I. (1980) *Eur. J. Biochem. 108*, 587–597.
Lowry, O., Rosebrough, N., Farr, A., & Randall, R. (1951) *J. Biol. Chem. 193*, 265.
Macura, S., & Ernst, R. R. (1980) *Mol. Phys. 41*, 95.
Merritt, E. A., Sundaralingam, M., Cornelius, R. D., & Cleland, W. W. (1978) *Biochemistry 17*, 3274.
Miara, J. E., Kang, J.-J., & Dahms, A. S. (1985) *Fourth International Conference on Na,K-ATPase* (Glynn, I., & Ellory, C., Eds.) p 109, Company of Biologists, Ltd., Cambridge, UK.
Mildvan, A. S. (1974) *Annu. Rev. Biochem. 43*, 357.
Mildvan, A. S. (1981) *Philos. Trans. R. Soc. London Ser. B. 293*, 65.
Mildvan, A., & Gupta, R. (1978) *Methods Enzymol. 49G*, 322–359.
Mildvan, A., Granot, J., Smith, G., & Liebman, M. (1980) *Adv. Inorg. Biochem. 2*, 211–236.
Noggle, J., & Schirmer, R. (1971) *The Nuclear Overhauser Effect*, pp 44–74, Academic Press, New York.
O'Connor, S., & Grisham, C. (1979) *Biochemistry 18*, 2315.
O'Connor, S., & Grisham, C. (1980) *FEBS Lett. 118*, 303.
Ohta, T., Yoshida, M., Nagano, K., Hirano, H., & Kawamura, M. (1986) *FEBS Lett. 204*, 297–301.
Olezniczak, E. T., Gampe, R. T., & Fesik, S. W. (1986) *J. Magn. Reson. 67*, 28.
Ovchinnikov, Y. A., Demin, V. V., Barnakov, A. N., Kuzin, A. P., Lunev, A. V., Modyanov, N. N., & Dzhandzhugazyan, K. N. (1985) *FEBS Lett. 190*, 73–76.
Perrin, C. L., & Gipe, R. K. (1984) *J. Am. Chem. Soc. 106*, 4036.
Rosevear, P., Bramson, H., O'Brian, C., Kaiser, E., & Mildvan, A. (1983) *Biochemistry 22*, 3439–3447.
Rosevear, P. R., Fox, T. L., & Mildvan, A. S. (1987a) *Biochemistry 26*, 3487–3493.
Rosevear, P. R., Powers, V., Dowhan, D., Mildvan, A. S., & Kenyon, G. L. (1987b) *Biochemistry 26*, 5338–5344.
Saenger, W. (1984) *Principles of Nucleic Acid Structure*, Springer-Verlag, New York.
Shull, G. E., & Lingrel, J. B. (1986) *J. Biol. Chem. 261*, 16788–16791.
Shull, G., Schwartz, A., & Lingrel, J. (1985) *Nature 316*, 691.
Skou, J. C. (1960) *Biochim. Biophys. Acta 42*, 6.
Sloan, D., & Mildvan, A. (1976) *J. Biol. Chem. 251*, 2412–2420.
Solomon, I. (1955) *Phys. Rev. 99*, 599.
States, D. J., Haberkorn, R. A., & Ruben, D. J. (1982) *J. Magn. Reson. 48*, 286.
Stewart, J., & Grisham, C. (1988) *Biochemistry 27*, 4840–4848.
Tribolet, R., Martin, R. B., & Sigel, H. (1987) *Inorg. Chem. 26*, 638.
Tropp, J., & Redfield, A. (1981) *Biochemistry 20*, 2133–2140.
Vilsen, B., Andersen, J. P., Petersen, J., & Jørgensen, P. L. (1987) *J. Biol. Chem. 262*, 10511–10517.
Viswamitra, M. A., Hosur, M. V., Shakked, Z., & Kennard, O. (1976) *Cryst. Struct. Commun. 5*, 819.